Author/s:
Cui, J;Björnmalm, M;Liang, K;Xu, C;Best, JP;Zhang, X;Caruso, F

Title:
Super-soft hydrogel particles with tunable elasticity in a microfluidic blood capillary model

Date:
2014-11-01

Citation:
Cui, J., Björnmalm, M., Liang, K., Xu, C., Best, J. P., Zhang, X. & Caruso, F. (2014). Super-soft hydrogel particles with tunable elasticity in a microfluidic blood capillary model. Advanced Materials, 26 (43), pp.7295-7299. https://doi.org/10.1002/adma.201402753.

Persistent Link:
https://hdl.handle.net/11343/113736

DOI: 10.1002/ ((please add manuscript number))
Article type: Communication

Super-Soft Hydrogel Particles with Tunable Elasticity in a Microfluidic Blood Capillary Model

*Jiwei Cui, Mattias Björnmalm, Kang Liang, Chenglong Xu, James P. Best, Xuehua Zhang, and Frank Caruso**

[*] Dr. J. Cui,[+] M. Björnmalm,[+] K. Liang, C. Xu, Dr. X. Zhang, Prof. F. Caruso
Department of Chemical and Biomolecular Engineering
The University of Melbourne
Parkville, Victoria 3010, Australia
E-mail: fcaruso@unimelb.edu.au

Dr. J. P. Best
Laboratory for Mechanics of Materials and Nanostructures, EMPA–Swiss Federal Laboratories for Materials Science and Technology, Feuerwerkerstrasse 39, 3602 Thun, Switzerland

[+] J. Cui and M. Björnmalm contributed equally to this work.

Keywords: PEG hydrogel particles, elasticity, mesoporous silica particles, microfluidic model, atomic force microscopy

Nanostructured polymer particles can be designed and engineered with a wide range of properties and can provide new and improved ways to diagnose and treat diseases.[1] The performance of nanostructured polymer particles in a biological setting is governed by their ability to interact with and address biological barriers.[2] Important factors determining this behavior include chemical and physical parameters, such as surface chemistry, size, shape, and elasticity.[3]

Different strategies have been investigated to avoid degradation and excretion of nanostructured particles. One prominent technique is the coating of particles with “stealth” materials such as poly(ethylene glycol) (PEG) or “self” peptides.[4] A high density stealth coating could improve penetration of large polymer particles and prolong their circulation time.[5] However, an incomplete or insufficient coating can limit the efficacy of such approaches.[6] A current challenge is accurately quantifying the surface coverage of stealth coatings on polymer particles.[7] One possible way to address this challenge is to assemble

particles solely made of materials such as PEG. Another important aspect of particle design is softness and deformability. Many mammalian cells have the remarkable capacity of reversible deformation. For example, human red blood cells (RBCs) have a mean diameter of ~7.5 μm and routinely traverse tissue blood capillaries with diameters that can be smaller than 5 μm.[8] Aged RBCs become rigid and lose this ability, which is reported to induce their clearance from the blood by splenic filtration.[9] Therefore, this flexibility is one of the key properties that enables long circulation of RBCs, and the reduced deformability is a characteristic of several pathological states.[10] It has been reported that the stiffness of nanoparticles plays an important role in their *in vivo* behavior: softer particles typically have longer circulation times and lower splenic accumulation.[11] Microfluidic devices have been recently used to mimic *in vivo* environments for studying the biological behavior of engineered particles.[12] Particles made of nanostructured materials that combine stealth properties with tunable mechanical properties are therefore of great interest for biological applications.

In the last few years, there have been several important steps made toward engineering soft particles with stealth properties. Using mixtures of diacrylated PEG with a photoinitiator and other acrylated polymers or PEG, templated or mask-based photopolymerization have been used to prepare hydrogel particles with tunable elasticity.[13] Such properties were achieved by varying the amount of diacrylated PEG used in prepolymer mixtures, as determined through electromechanical measurements on the bulk material and/or deformability behavior of particles inside designed microfluidic networks. Another route that has been explored is the use of layer-by-layer assembly to engineer particles that mimic RBCs.[14] Although these studies represent important advances, the particles were made of several components, including non-stealth components. In addition, the elasticity of the particles related to their behavior in microfluidic microchannels were only measured on the bulk material, rather than the particles. Furthermore, direct comparisons to the deformability behavior of RBCs in microfluidic channels were not reported.

Previously, we reported a robust approach for preparing polymer replica particles using a mesoporous silica (MS) templating method, where the template is removed following polymer infiltration and cross-linking.[15] This versatile method has been used to prepare particles of different size, shape, chemical composition, and elasticity, which have the capacity for both cargo encapsulation and delivery.[16] However, previous studies have not reported the preparation of stealth polymer replica particles with tunable elasticity.

Herein, we engineer PEG hydrogel particles with tunable elasticity and with a similar size to human RBCs via a MS templating method, followed by investigation of particle deformability using atomic force microscopy (AFM) and a microfluidic blood capillary model (**Scheme 1**). The particles consist solely of PEG, where 8-arm-PEG functionalized with amine (8-arm-PEG-NH_2) and succinimidyl carboxyl methyl ester (8-arm-PEG-NHS) were used as building blocks (Scheme 1b). The elastic modulus of the PEG particles is quantified using colloidal-probe atomic force microscopy (CP-AFM, Scheme 1c). Our method results in "super-soft" PEG particles, with more than 40-fold lower modulus than what has been previously reported for PEG-based hydrogel particles, and 130-fold lower modulus than human RBCs.[13b,c] Further, using a microfluidic blood capillary model that mimic dimensions and pressure differentials of the *in vivo* environment, we investigate the deformability behavior of these particles in microchannels and demonstrate that this behavior can be tuned to be similar to that of RBCs. This work demonstrates the nanoengineering of mechanically tunable super-soft hydrogel particles made solely out of the well-recognized stealth material PEG, which can provide improved ways of influencing and directing particle-cell interactions, biodistribution, and ultimately biological performance.

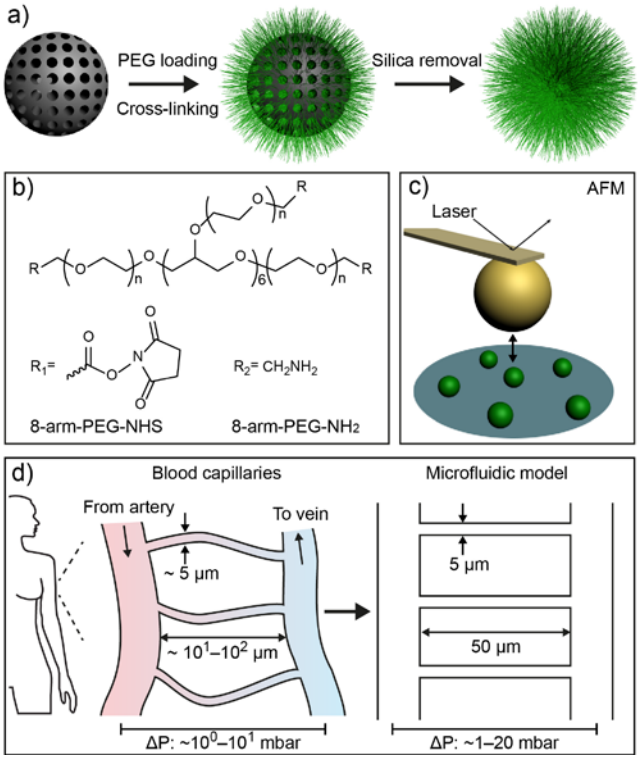

Scheme 1. a) Schematic illustration of the preparation of PEG particles via templating of MS particles. b) Molecular structure of 8-arm-PEG for the assembly of PEG particles. c) Schematic representation of the CP-AFM technique. d) The left scheme shows aspects of typical human blood capillaries. The right scheme shows a microfluidic blood capillary model, mimicking aspects of blood capillaries for investigation of capillary behavior of PEG particles.

For the construction of PEG particles, MS particles with an average size of 7.5 µm were used as templates (**Figure 1**a). To facilitate efficient PEG loading, 8-arm-PEG-NH_2 was used for infiltration into the MS templates based on electrostatic interactions between PEG and templates. The PEG particles were obtained though cross-linking the amine groups with 8-arm-PEG-NHS, followed by removal of the MS template (Scheme 1a). Cross-linker concentrations from 0.5 to 4 mg mL^{-1} were used, while concentrations below 0.5 mg mL^{-1} did not yield intact particles. For fluorescence imaging, Alexa Fluor 488 carboxylic acid, succinimidyl ester (AF488)-labeled 8-arm-PEG-NH_2 was used for the assembly of fluorescent

PEG particles. Figure 1b shows the obtained PEG particles dispersed in aqueous solution with a diameter around 7-9 μm, which is similar to that of RBCs (Figure 1c). The fluorescence intensity of the PEG particles increased when a higher concentration of cross-linker was used, as observed in Figure 1d. We speculate that more 8-arm-PEG-NH_2 was cross-linked in the particles as the concentration of 8-arm-PEG-NHS increased. That is, highly cross-linked PEG particles contained more polymer material. This is further supported by AFM and TEM imaging results (Figure S1). AFM images show a general trend of increasing height (from 25 ± 10, 45 ± 20, 300 ± 80 to 820 ± 100 nm) of the air-dried PEG particles with an increase of the 8-arm-PEG-NHS concentration from 0.5 to 4 mg mL^{-1}, while TEM images show that particles prepared with a higher concentration of 8-arm-PEG-NHS exhibit higher contrast.

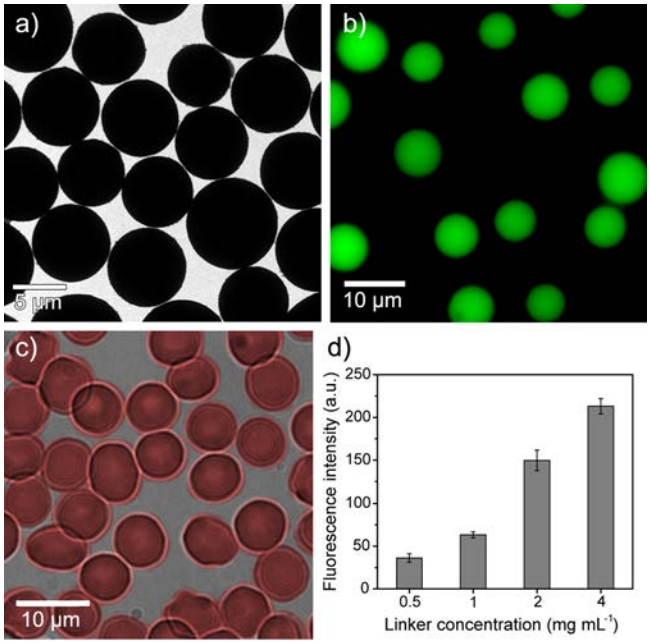

Figure 1. a) Transmission electron microscopy (TEM) image of SGX templates used for the assembly of PEG particles. b) Fluorescence microscopy image of AF488-labeled PEG particles cross-linked with 1 mg mL^{-1} of cross-linker. c) Bright-field microscopy image of RBCs (false colored). d) Fluorescence intensity of PEG particles as a function of cross-linker concentration.

In addition to the material type, the elasticity is also dependent on the material density. As the relative amount and/or density of PEG in each particle changed according to the amount of cross-linker used, we expected that the elasticity of the PEG particles would also vary with the cross-linker concentration. To measure the elasticity of the PEG particles, CP-AFM experiments were carried out.[17] High-resolution force maps were performed on single PEG particles with different cross-linking densities. CP-AFM measurements were performed on individual PEG particles dispersed in 20 mM phosphate buffer on a glass slide. An array of force curves were then collected over a 25 × 25 μm area, and then modified to give force-deformation information. Due to adhesive contact between the colloidal probe and particle, as well as possible viscoelastic effects and associated hysteresis, only the approach force curve was analyzed (**Figure 2**a). It was found that the Young's modulus (E_Y) of the PEG particles could be finely tuned by adjusting the cross-linker concentration (Figure 2b), which is consistent with our previous findings that the E_Y of poly(methacrylic acid) and poly(L-glutamic acid) particles increases with increasing the cross-linker concentration.[16c,18] However, the obtained PEG particles were super-soft with a tunable E_Y from 0.2 to 3.3 kPa (stiffness range from 0.3 to 3 mN m^{-1}), which is extremely low compared with previously reported polyelectrolyte particles (2-23 kPa), protein particles (~4 kPa) or PEG-based particles (7.8-64 kPa).[13b,16c,19] We hypothesize this is due to the low material density within the cross-linked structure.

E_Y values determined using JPK data processing software were arranged into a matrix and then graphically represented in three dimensions (Figure S2a-d). Based on the repetitive nature of the force mapping with little variability in elucidated modulus and height, it is seen that the PEG particles deformed elastically. From the force maps, E_Y values for the substrate have been removed for clarity, and it can be seen that there is a homogeneous region in the center of the particles, with decreasing modulus toward the edges due to edge effects during

compression. Additionally, the diameter of the PEG particles is much larger than that of the dispersed particles (7-9 µm), which can be explained by the radius of curvature (12.5 µm) for the spherical probe used (Figure S2e-h).

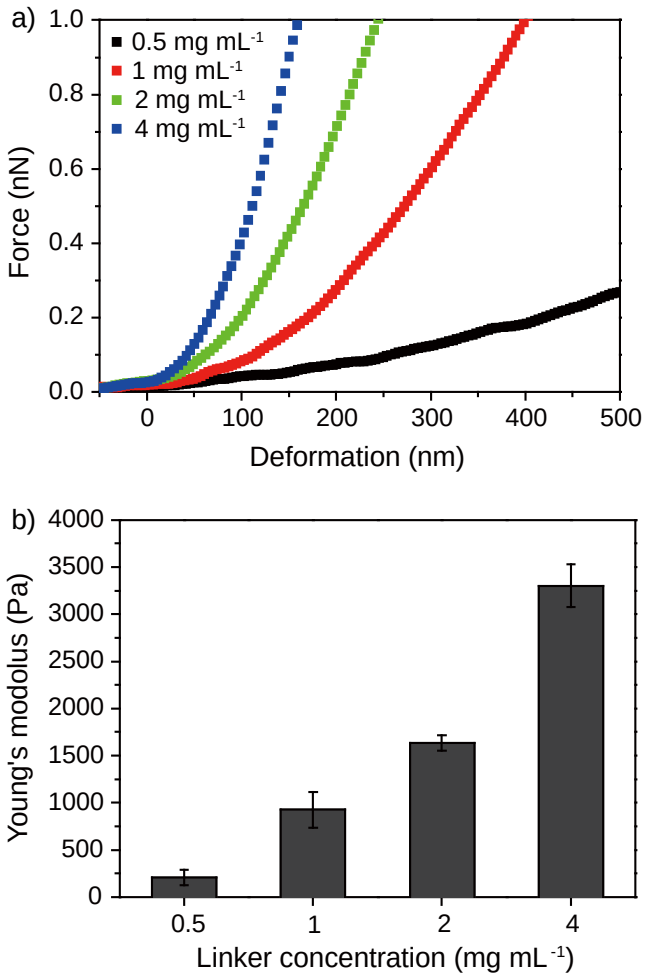

Figure 2. a) Representative F−δ curves for the PEG particles cross-linked with different cross-linker concentrations. b) Young's modulus (E_Y) derived from F−δ analysis for the PEG particles.

Human RBCs with a E_Y of ~26 kPa can easily pass through capillaries with dimensions smaller than their size and have a long circulation time *in vivo* (about 120 days).[11,20] As PEG particles are very soft (up to 130 times softer than RBCs), it was of interest to examine if they can behave like RBCs in hydrodynamic flow (e.g., narrow blood capillaries). To investigate the deformability of PEG particles in narrow capillaries, we designed a microfluidic blood capillary model. Finite element simulations (COMSOL Multiphysics 4.3) were performed using different parameters and the design was refined until physiologically relevant results were obtained (**Figure 3**a). Here, pressure drops (2–20 mbar) were established over the microchannels, which are comparable to the *in vivo* pressure drops across typical human blood capillaries (~1-10 mbar).[21] The parameters for the simulations of flow in the microfluidic device are listed in Table S1. The refined and validated design was then realized using soft lithography (Figure 3b) and consisted of a high-pressure and a low-pressure side connected by many microchannels in parallel, similar to the *in vivo* environment where a high-pressure arterial side is connected to a low-pressure venous side through capillary networks. This four-point device design (two inlets, two outlets) facilitates the establishment of well-controlled differential pressures and pressure drops across the microchannels (as the pressure on each side can be tuned independently). Figure 3c shows a scanning electron microscopy (SEM) image of the central microchannels (width 5 μm, height 12 μm) in the microfluidic device.

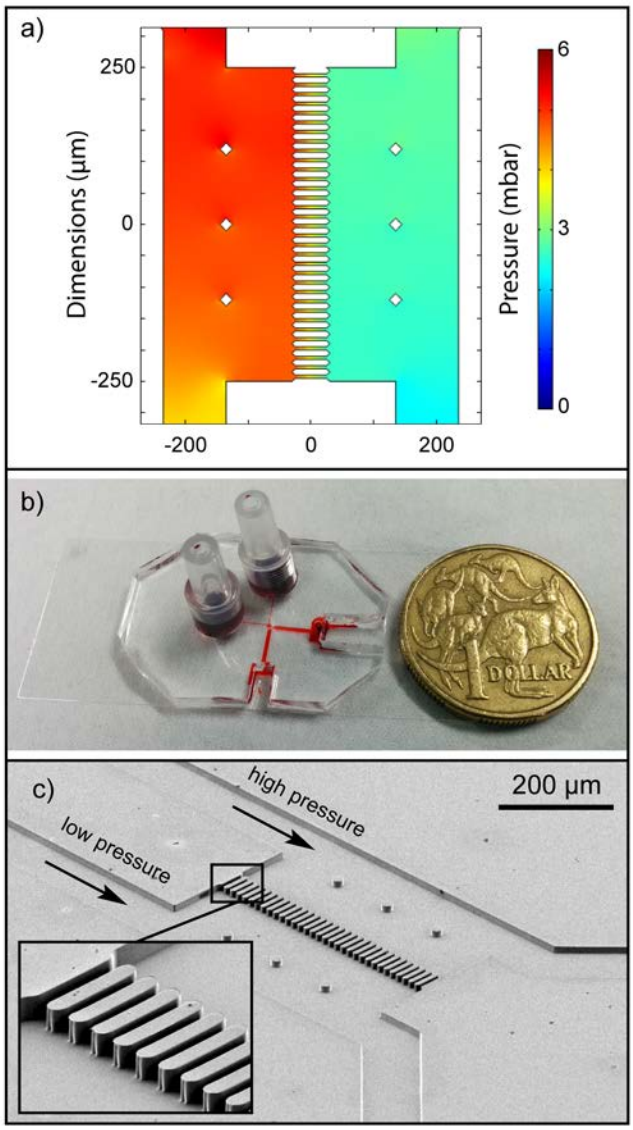

Figure 3. a) Finite-element analysis based simulations of microfluidic device to investigate pressure differentials. In this example, 20 and 10 mbar was used for the high and low pressure inlets, respectively, resulting in a pressure drop across the microchannels of ~2.2 mbar. b) Photograph of the microfluidic device. Red dye was used to emphasize the microfluidic channels. c) SEM image of a PDMS microfluidic device. The inset shows a higher magnification image of the smallest features of the device.

To test the deformability behavior of PEG particles in capillaries, the inlet pressures were chosen based on the simulations to achieve physiologically relevant pressure drops across the

microchannels. The PEG particles were injected from the high pressure inlet and only buffer was used in the second inlet. The highly cross-linked PEG particles had trouble passing through the microchannels, especially at lower pressure differentials (**Figure 4**a). In contrast, lowly cross-linked PEG particles could more easily deform to fit inside the microchannels and pass through (Figure 4b). Interestingly, no damage to the spherical shape was observed when comparing PEG particles before and after passing through the microchannels. This indicates that PEG particles can pass through microchannels that are smaller than the particle diameter through reversible elastic deformation. As a comparison, human RBCs were also tested in the microfluidic blood capillary model. They could also pass through the microchannels and recover their shape, as expected (Figure 4c).[8,22]

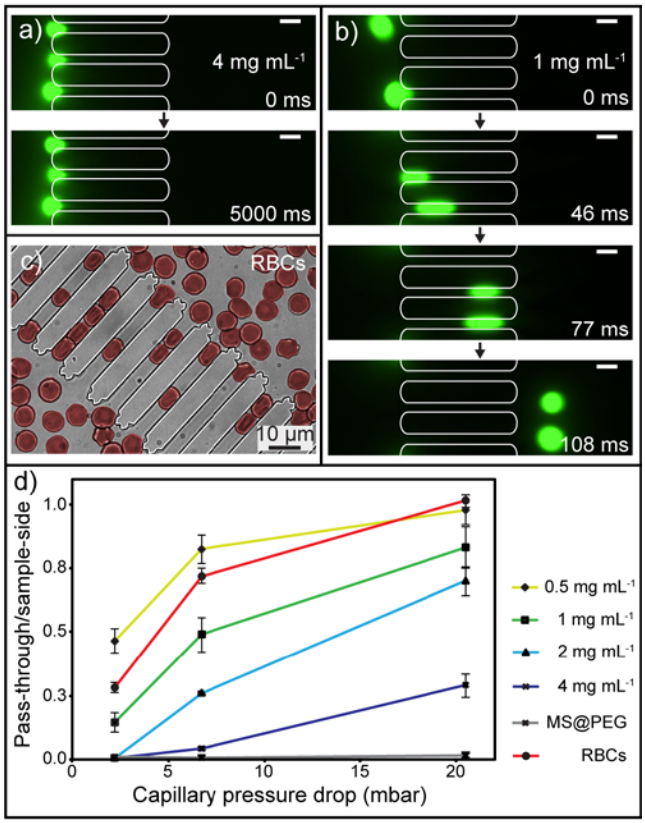

Figure 4. a,b) Time-lapse fluorescence microscopy images of particles (green) stopping (cross-linker concentration of 4 mg ml^{-1}) or passing through (cross-linker concentration of 1 mg ml^{-1}) the capillaries. Outline of capillaries from bright-field and overlayed. c) Bright-field

microscopy image of RBCs (colored red) passing through capillaries. Scale bars, 10 µm. The pressure drop in the microchannels is ~6 mbar in (a-c). d) Particle trajectory analysis of particles (cross-linker concentration of 0.5–4 mg ml^{-1}) and controls (MS@PEG and RBCs). Number of particles that passed through the capillaries was divided by the number that went to the outlet on the same side. Mean ± standard deviation, n = 3.

To quantify the deformability of the PEG particles with different cross-linking densities in microchannels, a ratio of the number of particles that passed through the microchannels to the number of particles that did not was calculated. Particles that can easily pass through will have a high ratio while particles that do not pass through at all will have a ratio of zero. Each measurement was performed in triplicate with more than 100 particle trajectories analyzed for each replicate. In total over 20,000 particle trajectories were analyzed. The results demonstrate a clear inverse correlation between amount of cross-linker used and the ease with which particles can pass through the microchannels (Figure 4d). This correlates well with the AFM data (Figure 2), where a decrease in cross-linker used resulted in a decrease in $E_{Y,}$ corresponding to an increase in softness, which here translates to an increased capacity to deform to pass through the microchannels. Further, the PEG particles pass through the microchannels more easily when the pressure drops increased, as expected. Virtually none of the control PEG particles with the hard MS template still remaining (MS@PEG) could pass through the microchannels, even at the highest pressure differential used, as expected. Interestingly, when the linker concentration decreased to 0.5 mg mL^{-1}, the lowly cross-linked PEG particles with an E_Y of 0.2 kPa behaved similar to RBCs in the microfluidic blood capillary model. It should be noted that even though the E_Y of highly cross-linked PEG particles is still lower than that of RBCs, they do not pass through the capillary model as well as RBCs. This is due to a combination of geometric differences between biconcave-discoidal RBCs and spherical PEG particles with distinct internal volumes, along with effects from the

RBC cytoplasmic viscosity and contrasts in mechanical deformation of the respective membranes.[20,23] Nevertheless, the obtained PEG particles demonstrate tunable elasticity and they can be made to behave similar to RBCs under physiologically relevant conditions in a microfluidic blood capillary model, thus making them potentially useful for biomedical applications, such as targeted drug delivery.

In summary, super-soft hydrogel particles made of 8-arm-PEG were successfully fabricated via a MS templating method. These PEG particles were well dispersed in aqueous solution and had a size similar to RBCs. The cross-linking density of the PEG particles increased as the concentration of cross-linker used increased. It was found that the E_Y of the PEG particles, as quantified with CP-AFM, could be tailored from 0.2 to 3.3 kPa by increasing the cross-linker concentration from 0.5 to 4 mg mL^{-1}. A microfluidic blood capillary model was used to investigate the behavior of PEG particles in a physiologically relevant flow environment. It was found that the deformability behavior and ability to pass through microchannels could be tuned through the cross-linking concentration, and that this behavior could be tailored to be similar to that of human RBCs. The reported PEG particles represent a new generation of soft hydrogel particles for investigating particle behavior in biological environments, which have the potential to provide new insights for the design and development of improved drug delivery carriers for biomedical applications.

Experimental section

Materials: 8-arm-PEG-NH_2 (40 kDa) and 8-arm-PEG-NHS (10 kDa) with hexaglycerol core structure were purchased from JenKem Technology USA Inc (China) and Creative PEGWorks (USA), respectively. Mesoporous silica (MS) particles (Separon SGX 200, average diameter 7.5 µm, pore size 20 nm) were obtained from Tessek Ltd (Czech Republic).

Fabrication of PEG particles: MS particles were incubated overnight in 8-arm-PEG-NH_2 solution (5 mg mL^{-1} in phosphate buffer) under constant shaking. After washing, the pellet

was redispersed in 8-arm-PEG-NHS solution at different concentrations (0.5, 1, 2, or 4 mg mL^{-1} in phosphate buffer) and incubated for at least 2 h. After washing, the MS templates were removed with 2 M HF/8 M NH_4F solution (pH ~5). *Caution! HF is highly toxic. Extreme care should be taken when handling HF solution*. The resultant PEG particles were washed and redispersed in water. For fluorescence imaging, 8-arm-PEG-NH_2 was pre-labeled with AF488.

Characterization Methods: Images were acquired using transmission electron microscopy (Philips CM120 BioTWIN), atomic force microscopy (NanoWizard II AFM) and fluorescence microscopy (Olympus IX71). Fluorescence intensity of PEG particles were measured on an Apogee Micro Flow Cytometer. Mechanical characterization of the PEG particles was performed using a Nanowizard II AFM equipped with a fluorescence microscope (Leica DMI4000B).[24] The microfluidic model mimicking aspects of human blood capillaries was made through soft lithography.[25]

Full experimental details are available in the Supporting Information.

Supporting Information

Supporting Information is available from the Wiley Online Library or from the author.

Acknowledgements

This research was conducted and funded by the Australian Research Council Centre of Excellence in Convergent Bio-Nano Science and Technology (project number CE140100036). This work was also supported by the Australian Research Council under the Australian Laureate Fellowship (F.C., FL120100030) and the Super Science Fellowship (F.C., FS110200025) schemes, as well as the Australian Government through an International Postgraduate Research Scholarship (M.B.) and an Australian Postgraduate Award (M.B.). K.L. acknowledges the CSIRO OCE Postdoctoral Fellowship and Science Leader schemes.

J.P.B. acknowledges funding from the EMPA Postdoc program co-funded by FP7:Marie Curie Actions. This work was performed in part at both the Melbourne Centre for Nanofabrication in the Victorian Node and at the Optofab Node of the Australian National Fabrication Facility, and in part at the Advanced Fluorescence Imaging Platform at the Melbourne Materials Institute, The University of Melbourne. Christian Löbbe is thanked for the help of force spectroscopy measurements and analysis. J. Cui and M. Björnmalm contributed equally to this work.

Received: ((will be filled in by the editorial staff))
Revised: ((will be filled in by the editorial staff))
Published online: ((will be filled in by the editorial staff))

References

[1] a) G. Bao, S. Mitragotri, S. Tong, *Annu. Rev. Biomed. Eng.* **2013**, *15*, 253; b) S. Mura, J. Nicolas, P. Couvreur, *Nat. Mater.* **2013**, *12*, 991; c) E. K. H. Chow, D. Ho, *Sci. Transl. Med.* **2013**, *5*, 216rv4; d) Y. Yan, M. Björnmalm, F. Caruso, *ACS Nano* **2013**, *7*, 9512.

[2] a) V. P. Chauhan, R. K. Jain, *Nat. Mater.* **2013**, *12*, 958; b) Y. Yan, M. Björnmalm, F. Caruso, *Chem. Mater.* **2014**, *26*, 452; c) M. J. Ernsting, M. Murakami, A. Roy, S. D. Li, *J. Control. Release* **2013**, *172*, 782.

[3] a) A. Albanese, P. S. Tang, W. C. W. Chan, *Annu. Rev. Biomed. Eng.* **2012**, *14*, 1; b) R. A. Petros, J. M. DeSimone, *Nat. Rev. Drug Discovery* **2010**, *9*, 615.

[4] a) P. L. Rodriguez, T. Harada, D. A. Christian, D. A. Pantano, R. K. Tsai, D. E. Discher, *Science* **2013**, *339*, 971; b) K. Knop, R. Hoogenboom, D. Fischer, U. S. Schubert, *Angew. Chem. Int. Ed.* **2010**, *49*, 6288.

[5] a) E. A. Nance, G. F. Woodworth, K. A. Sailor, T.-Y. Shih, Q. Xu, G. Swaminathan, D. Xiang, C. Eberhart, J. Hanes, *Sci. Transl. Med.* **2012**, *4*, 149ra119; b) J. M. Rabanel, P. Hildgen, X. Banquy, *J. Control. Release* **2014**, *185*, 71.

[6] J. V. Jokerst, T. Lobovkina, R. N. Zare, S. S. Gambhir, *Nanomedicine* **2011**, *6*, 715.

[7] a) J. L. Perry, K. G. Reuter, M. P. Kai, K. P. Herlihy, S. W. Jones, J. C. Luft, M. Napier, J. E. Bear, J. M. DeSimone, *Nano Lett.* **2012**, *12*, 5304; b) Q. Yang, S. W. Jones, C. L. Parker, W. C. Zamboni, J. E. Bear, S. K. Lai, *Mol. Pharmaceutics* **2014**, *11*, 1250.

[8] R. Skalak, P. Branemark, *Science* **1969**, *164*, 717.

[9] R. E. Mebius, G. Kraal, *Nat. Rev. Immunol.* **2005**, *5*, 606.

[10] F. C. Mokken, M. Kedaria, C. P. Henny, M. R. Hardeman, A. W. Gelb, *Ann. Hematol.* **1992**, *64*, 113.

[11] L. Zhang, Z. Cao, Y. Li, J.-R. Ella-Menye, T. Bai, S. Jiang, *ACS Nano* **2012**, *6*, 6681.

[12] M. Björnmalm, Y. Yan, F. Caruso, *J. Control. Release*, DOI: 10.1016/j.jconrel.2014.04.030.

[13] a) R. Haghgooie, M. Toner, P. S. Doyle, *Macromol. Rapid Commun.* **2010**, *31*, 128; b) T. J. Merkel, S. W. Jones, K. P. Herlihy, F. R. Kersey, A. R. Shields, M. Napier, J. C. Luft, H. Wu, W. C. Zamboni, A. Z. Wang, J. E. Bear, J. M. DeSimone, *Proc. Natl. Acad. Sci. U.S.A.* **2011**, *108*, 586; c) K. Chen, T. J. Merkel, A. Pandya, M. E. Napier, J. C. Luft, W. Daniel, S. Sheiko, J. M. DeSimone, *Biomacromolecules* **2012**, *13*, 2748.

[14] a) N. Doshi, A. S. Zahr, S. Bhaskar, J. Lahann, S. Mitragotri, *Proc. Natl. Acad. Sci. U.S.A.* **2009**, *106*, 21495; b) S. P. She, Q. Q. Li, B. W. Shan, W. J. Tong, C. Y. Gao, *Adv. Mater.* **2013**, *25*, 5814.

[15] Y. Wang, A. Yu, F. Caruso, *Angew. Chem. Int. Ed.* **2005**, *117*, 2948.

[16] a) Y. Wang, F. Caruso, *Chem. Mater.* **2006**, *18*, 4089; b) J. Cui, Y. Yan, Y. Wang, F. Caruso, *Adv. Funct. Mater.* **2012**, *22*, 4718; c) J. Cui, R. De Rose, J. P. Best, A. P. R. Johnston, S. Alcantara, K. Liang, G. K. Such, S. J. Kent, F. Caruso, *Adv. Mater.* **2013**, *25*, 3468.

[17] a) S. Schmidt, P. A. Fernandes, B. G. De Geest, M. Delcea, A. G. Skirtach, H. Möhwald, A. Fery, *Adv. Funct. Mater.* **2011**, *21*, 1411; b) A. Fery, R. Weinkamer, *Polymer* **2007**, *48*, 7221.

[18] J. P. Best, J. Cui, M. Müllner, F. Caruso, *Langmuir* **2013**, *29*, 9824.

[19] S. Schmidt, M. Behra, K. Uhlig, N. Madaboosi, L. Hartmann, C. Duschl, D. Volodkin, *Adv. Funct. Mater.* **2013**, *23*, 116.

[20] I. Dulińska, M. Targosz, W. Strojny, M. Lekka, P. Czuba, W. Balwierz, M. Szymoński, *J. Biochem. Bioph. Methods* **2006**, *66*, 1.

[21] Y. C. Fung, B. W. Zweifach, *Annu. Rev. Fluid Mech.* **1971**, *3*, 189.

[22] a) J. L. McWhirter, H. Noguchi, G. Gompper, *Proc. Natl. Acad. Sci. U.S.A.* **2009**, *106*, 6039; b) H. Noguchi, G. Gompper, *Proc. Natl. Acad. Sci. U.S.A.* **2005**, *102*, 14159.
[23] N. Mohandas, J. A. Chasis, *Semin. Hematol.* **1993**, *30*, 171.
[24] J. P. Best, M. P. Neubauer, S. Javed, H. H. Dam, A. Fery, F. Caruso, *Langmuir* **2013**, *29*, 9814.
[25] D. Qin, Y. N. Xia, G. M. Whitesides, *Nat. Protoc.* **2010**, *5*, 491.